

## Deactivation Behavior and Excited-State Properties of (Coumarin-4-yl)methyl Derivatives. 2. Photocleavage of Selected (Coumarin-4-yl)methyl-Caged Adenosine Cyclic 3',5'-Monophosphates with Fluorescence Enhancement

Torsten Eckardt,<sup>†</sup> Volker Hagen,<sup>†</sup> Björn Schade,<sup>†</sup> Reinhardt Schmidt,<sup>‡</sup> Claude Schweitzer,<sup>‡</sup> and Jürgen Bendig\*<sup>§</sup>

*Institute of Molecular Pharmacology, Robert-Rössle-Strasse 10, D-13125 Berlin, Germany, Institute of Physical and Theoretical Chemistry, Johann-Wolfgang-Goethe University Frankfurt/Main, D-60439 Frankfurt/Main, Germany, and Institute of Chemistry, Humboldt University Berlin, Hessische Strasse 1-2, D-10115 Berlin, Germany*

juergen=bendig@chemie.hu-berlin.de

Received July 10, 2001

A series of axial and equatorial diastereomers of (coumarin-4-yl)methyl-caged adenosine cyclic 3',5'-monophosphates (cAMPs), **1–6**, having methoxy, dialkylamino, or no substituent in the 6- and/or 7-positions, and their corresponding 4-(hydroxymethyl)coumarin photoproducts **7–12** have been synthesized. The photochemical and UV/vis spectroscopical properties (absorption and fluorescence) of **1–6** and **7–12** have been examined in methanol/aqueous HEPES buffer solution. Donor substitution in the 6-position causes a strong bathochromic shift of the long-wavelength absorption band, whereas substitution in the 7-position leads only to a weak red shift. The photochemical cleavage of the caged cAMPs was investigated, and the photoproducts were analyzed. Photochemical quantum yields, fluorescence quantum yields, and lifetimes of the excited singlet states were determined. The highest values of photochemical quantum yields (photo-S<sub>N</sub>1 mechanism) were obtained with caged cAMPs having a donor substituent in the 7-position of the coumarin moiety, caused by electronic stabilization of the intermediately formed coumarinylmethyl cation. With donor substitution in the 6-position, the resulting moderate electronic stabilization of the coumarinylmethyl cation is overcompensated by the strong bathochromic shift, reducing the energy gap between the excited-state S<sub>1</sub> and the corresponding coumarinylmethyl cation. The rate constant for the ester cleavage and liberation of cAMP is about 10<sup>9</sup> s<sup>-1</sup>, estimated for the axial isomer of **6** by analysis of the fluorescence increase of the alcohol **12** formed upon laser pulse photolysis.

### Introduction

The controlled photochemical release of bioactive effector molecules from masked inactive derivatives (caged compounds) represents an exceptional method for investigating the mechanisms and kinetics of biomolecular processes inside living cells.<sup>1,2</sup> This technique allows the generation of instantaneous concentration increases of the biomolecule in the vicinity of activity, and the biological response is triggered almost without delay.

Several investigators have successfully employed caged adenosine cyclic 3',5'-monophosphates (cAMPs) to study cAMP-dependent cellular processes.<sup>2–4</sup> Recently Furuta et al. introduced (7-methoxycoumarin-4-yl)methyl-caged cAMP (7-MCM-caged cAMP) and described its favorable properties such as a long half-life in the dark in physiological buffer solutions and its relatively high efficiency of photorelease.<sup>5</sup> Using time-resolved fluorescence measurements, we recently found that the analogues 7-MCM-caged 8-Br-cAMP and 7-MCM-caged 8-Br-cGMP released the corresponding cyclic nucleotides (8-Br-cAMP, 8-Br-cGMP) rapidly within a few nanoseconds.<sup>6</sup> The photocleavage (Scheme 1) was shown to proceed similarly to that of naphthylalkyl<sup>7,8</sup> and benzyl<sup>9</sup> phosphates and involves heterolysis of the C–O ester bond (solvent-

\* To whom correspondence should be addressed.

<sup>†</sup> Institute of Molecular Pharmacology.

<sup>‡</sup> Johann-Wolfgang-Goethe University Frankfurt/Main.

<sup>§</sup> Humboldt University Berlin.

(1) (a) Lester, H. A.; Nerbonne, J. M. *Annu. Rev. Biophys. Bioeng.* **1982**, *11*, 151–175. (b) Nerbonne, J. M. In *Optical Methods in Cell Physiology*; De Weer, P., Salzberg, B. M., Eds.; Wiley: New York, 1986; Vol. 40, pp 417–445. (c) Gurney, A. M.; Lester, H. A. *Physiol. Rev.* **1987**, *67*, 583–617. (d) McCray, J. A.; Trentham, D. R. *Annu. Rev. Biophys. Chem.* **1989**, *18*, 239–270. (e) Wootton, J. F.; Trentham, D. R. In *Photochemical Probes in Biochemistry*; Nielsen, P. E., Ed.; NATO ASI Series C; Kluwer Academic: Dordrecht, The Netherlands, **1989**; Vol. 272, pp 277–296. (f) Kaplan, J. H.; Somlyo, A. P. *Trends Neurosci.* **1989**, *12*, 54–58. (g) Adams, S. R.; Tsien, R. Y. *Annu. Rev. Physiol.* **1993**, *55*, 755–784. (h) Corrie, J. E. T.; Trentham, D. R. In *Bioorganic Photochemistry*; Morrison, H., Ed.; Wiley: New York, 1993; Vol. 2, pp 243–305. (i) Kao, J. P. Y.; Adams, S. R. *Optical Microscopy: Emerging Methods and Applications*; Academic Press: San Diego, 1993; pp 27–85.

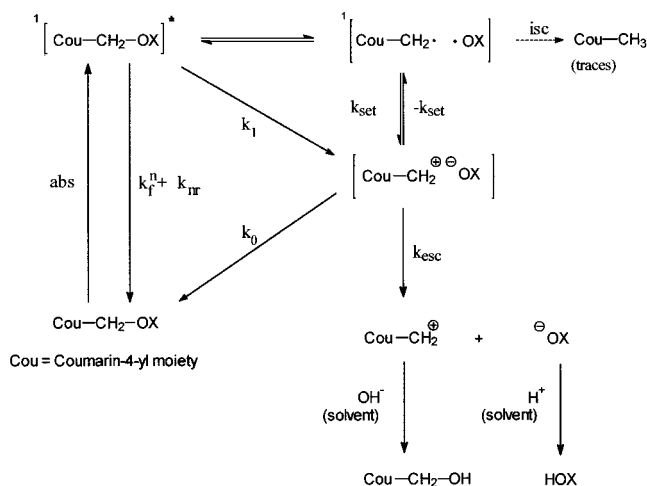
(2) (a) Hagen, V.; Dzeja, C.; Bendig, J.; Baeger, I.; Kaupp, U. B. *J. Photochem. Photobiol., B* **1997**, *42*, 71–78. (b) Hagen, V.; Dzeja, C.; Frings, S.; Bendig, J.; Krause, E.; Kaupp, U. B. *Biochemistry* **1996**, *35*, 7762–7771.

(3) Walker, J. W.; Reid, G. P.; Trentham, D. R. *Methods Enzymol.* **1989**, *172*, 288–301.

(4) (a) Korth, M.; Engels, J. *Naunyn-Schmiedeberg's Arch. Pharmacol.* **1979**, *310*, 103–111. (b) Nargeot, J.; Nerbonne, J. M.; Engels, J.; Lester, H. A. *Proc. Natl. Acad. Sci. U.S.A.* **1983**, *80*, 2395–2399. (c) Nerbonne, J. M.; Richard, S.; Nargeot, J.; Lester, H. A. *Nature* **1984**, *310*, 74–76. (d) Wiesner, B.; Hagen, V. *J. Photochem. Photobiol., B* **1999**, *49*, 112–119. (e) Frings, S.; Hackos, D. H.; Dzeja, C.; Okyama, T.; Hagen, V.; Kaupp, U. B.; Korenbrot, J. *Methods Enzymol.* **2000**, *315*, 797–817.

(5) (a) Furuta, T.; Torigai, H.; Sugimoto, M.; Iwamura, M. *J. Org. Chem.* **1995**, *60*, 3953–3956. (b) Furuta, T.; Iwamura, M. *Methods Enzymol.* **1998**, *291*, 50–63.

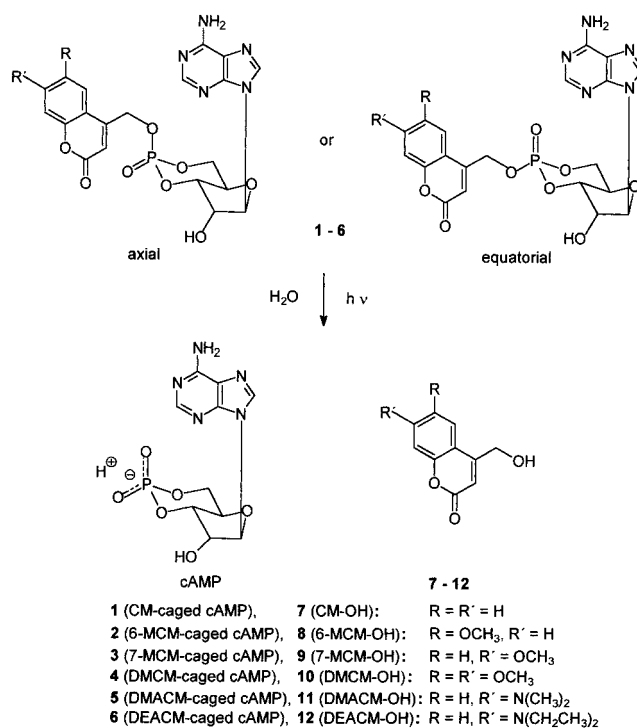
(6) Hagen, V.; Bendig, J.; Frings, S.; Wiesner, B.; Schade, B.; Helm, S.; Lorenz, D.; Kaupp, U. B. *J. Photochem. Photobiol., B* **1999**, *53*, 91–102.

**Scheme 1. Mechanism of the Photolysis of Caged cAMPs 1–6**

assisted photoheterolysis) and subsequent ion-pair separation by the polar solvent (formation of cAMP), followed by trapping of the coumarinylmethyl carbocation by the solvent (hydroxylation).<sup>10</sup> This ionic mechanism is inconsistent with the radical pathway postulated by Furuta<sup>11</sup> for (7-methoxycoumarin-4-yl)methyl diethyl phosphate. Furthermore, we reported that 7-MCM-caged cyclic nucleotides are only weakly fluorescent, whereas the photoproduct 4-(hydroxymethyl)-7-methoxycoumarin (7-MCM-OH) shows strong fluorescence, which should facilitate monitoring of the release process.<sup>6,10,12</sup>

In this paper we investigate the influence of substituents in the 6- and 7-positions of the coumarin caging group on (i) the spectroscopic properties (absorption and fluorescence), (ii) the photophysical deactivation behavior (fluorescence ability), and (iii) the photochemical reactions of caged cAMPs.

Substituents influence the absorption and fluorescence band positions of coumarin derivatives.<sup>13,14</sup> Electron-donating substituents in the 6- and/or 7-positions and electron-withdrawing substituents in the 3-position of the 4-methylcoumarin moiety cause a significant bathochromic shift of the  $S_0$ - $S_1$  transition. Most of the substituted coumarins are characterized by large fluorescence quan-

**Scheme 2. Photolysis of the Axial and Equatorial Isomers of (Coumarin-4-yl)methyl Esters of cAMP (1–6), Liberating the (Coumarin-4-yl)methyl Alcohols 7–12 and cAMP**

tum yields. In the absence of heavy atoms<sup>15</sup> and for the 6- and 8-bromo-substituted coumarins,<sup>16</sup> the triplet population is negligible and fluorescence competes with the nonradiative deactivation (internal conversion).<sup>10</sup> The weak fluorescence is explained by an accelerated internal conversion from the excited state caused by mixing of the  $\pi\pi^*$  and the  $n\pi^*$  states.<sup>10,14</sup> Additionally, the low fluorescence quantum yields of some donor-acceptor-substituted coumarins are explained by a nonradiative deactivation pathway via a twisted intramolecular charge-transfer (TICT) state.<sup>16</sup> Surprisingly, the influence of coumarin structure on the efficiency of the photochemical bond cleavage has not been investigated so far.

Photoactivation of the (coumarin-4-yl)methyl esters of cAMP (**1–6**) leads to the corresponding 4-(hydroxymethyl)coumarins **7–12**, which are liberated during photolysis of the phototrigger compounds (Scheme 2). To study the influence of the electronic properties of donor substituents on the spectroscopic characteristics and photochemical efficiency, we synthesized the axial and equatorial isomers of (coumarin-4-yl)methyl esters of cAMP (**1–6**) (Scheme 3). **6** was already described in connection with another series of caged cAMPs.<sup>13i</sup> In addition, the corresponding 4-(hydroxymethyl)coumarins **7–12** were prepared to investigate the photophysical deactivation behavior (Table 1). Furthermore, the phototriggers **2–4** and their corresponding alcohols **8–10** were selected to determine the influence of the number and position of the substituents. Our final goal was to design suitable (coumarin-4-yl)methyl-caged cAMPs with strong long-wavelength absorption bands, high photochemical quantum yields, and strong fluorescence enhancement during photolysis.

(7) (a) Itoh, Y.; Gouki, M.; Goshima, T.; Hachimori, A.; Kojima, M.; Karatsu, T. *J. Photochem. Photobiol., A* **1998**, *117*, 91–98. (b) Pincock, J. A. *Acc. Chem. Res.* **1997**, *30*, 43–49. (c) Arnold, B.; Donald, L.; Jurgens, A.; Pincock, J. A. *Can. J. Chem.* **1985**, *63*, 3140–3146.

(8) Givens, R. S.; Matuszewski, B. *J. Am. Chem. Soc.* **1984**, *106*, 6860–6861.

(9) Hillborn, J. W.; MacKnight, E.; Pincock, J. A.; Wedge, P. J. *J. Am. Chem. Soc.* **1994**, *116*, 3337–3346.

(10) Schade, B.; Hagen, V.; Schmidt, R.; Herbrich, R.; Krause, E.; Eckardt, T.; Bendig, J. *J. Org. Chem.* **1999**, *64*, 9109–9117.

(11) Furuta, T.; Wang, S. S.-H.; Dantzker, J. L.; Dore, T. M.; Bybee, W. J.; Callaway, E. M.; Denk, W.; Tsen, R. Y. *Proc. Natl. Acad. Sci. U.S.A.* **1999**, *96*, 1193–1200.

(12) Bendig, J.; Helm, S.; Hagen, V. *J. Fluoresc.* **1997**, *7*, 357–361.

(13) (a) Ito, K.; Maruyama, J. *Chem. Pharm. Bull.* **1983**, *31*, 3014–3023. (b) Giri, R.; Rathi, S. S.; Machwe, M. K.; Murti, V. V. S. *Spectrochim. Acta* **1988**, *44A*, 805–807. (c) Arbeola, T. L.; Arbeola, F. L.; Tapia, M. J.; Arbeola, I. L. *J. Phys. Chem.* **1993**, *97*, 4704–4707. (d) Rechthaler, K.; Köhler, G. *Chem. Phys.* **1994**, *189*, 99–116. (e) Kaholek, M.; Hrdlovic, P. *J. Photochem. Photobiol., A* **1997**, *108*, 283–288. (f) Raju, B. B.; Eliasson, B. *J. Photochem. Photobiol., A* **1998**, *116*, 135–142. (g) Fabian, W. M. F.; Niederreiter, K. S.; Uray, G.; Stadlbauer, W. *J. Mol. Struct.* **1999**, *477*, 209–220. (h) Joshi, H. S.; Jamshidi, R.; Tor, Y. *Angew. Chem.* **1999**, *111*, 2888–2891. (i) Hagen, V.; Bendig, J.; Frings, S.; Eckardt, T.; Helm, S.; Reuter, D.; Kaupp, U. B. *Angew. Chem., Int. Ed.* **2001**, *40*, 1046–1048.

(14) Seixas de Melo, J. S.; Becker, R. S.; Macanita, A. L. *J. Phys. Chem.* **1994**, *98*, 6054–6058.

(15) Li, L.-D.; Yang, S.-Z. *Anal. Chim. Acta* **1994**, *296*, 99–105.

(16) Corrie, J. E. T.; Munasinghe, V. R. N.; Rettig, W. *J. Heterocycl. Chem.* **2000**, *37*, 1447–1455.

**Scheme 3. Synthesis of the Axial and Equatorial Isomers of (Coumarin-4-yl)methyl Esters of cAMP (1–6)**

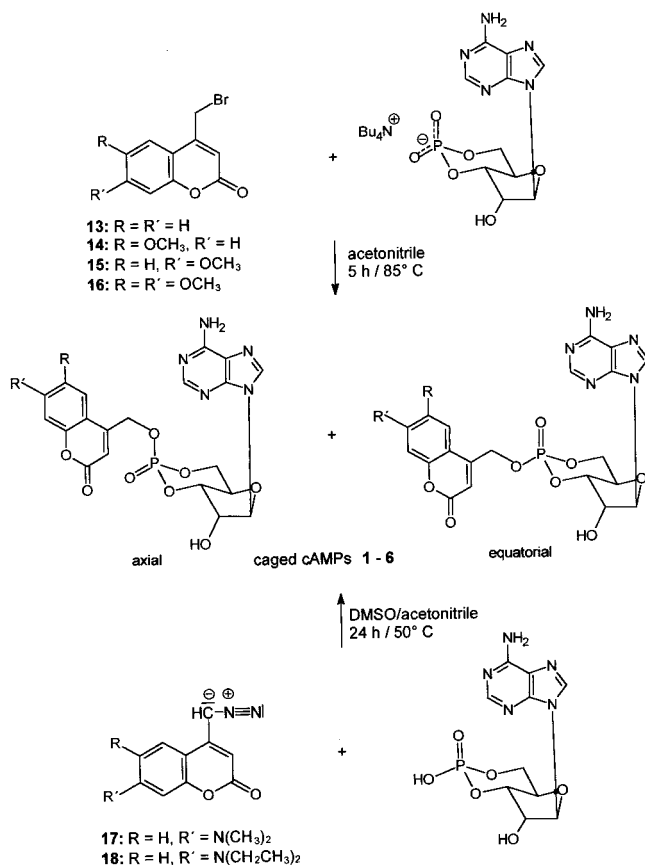


**Table 1. Photophysical Data of the (Coumarin-4-yl)methyl Alcohols 7–12 in MeOH/HEPES, 1:4**

compound	$\tau_f$ /ns	$\tau_f^{\text{fl}}$ /ns	$k_f$ /(10 <sup>8</sup> s <sup>-1</sup> )
CM-OH (7)	<0.4	<80	>0.125
6-MCM-OH (8)	2.67	16.7	0.6
7-MCM-OH (9)	3.5	5.4	1.86
DMCM-OH (10)	4.9	8.3	1.20
DMACM-OH (11)	3.42	5.66	1.77
DEACM-OH (12)	3.35	4.93	2.03

### Results and Discussion

**Synthesis.** The caged cAMPs 1–4 were synthesized by two different methods, involving substitution of the respective 4-(bromomethyl)coumarins using either the tetra-*n*-butylammonium salt of cAMP following our recently developed approach<sup>6,10</sup> (Scheme 3) or silver(I) oxide activated cAMP as described by Furuta et al.<sup>5,17</sup> Among the advantages of the tetra-*n*-butylammonium salt procedure are higher product yields, shorter reaction times, larger diastereomeric excess of the axial isomers of caged cAMPs 1–4, and facilitated workup in comparison with the silver(I) oxide route.<sup>10</sup> Contrary to the preparation of 1–4, attempts to obtain (7-(dialkylamino)coumarin-4-yl)methyl-caged cAMPs 5 and 6 under these reaction conditions failed. These caged cAMP derivatives were therefore synthesized by alkylation of the free acid of cAMP with 4-(diazomethyl)-7-(dimethylamino)coumarin (17) and 4-(diazomethyl)-7-(diethylamino)coumarin (18)

(17) Furuta, T.; Torigai, H.; Osawa, T.; Iwamura, M. *J. Chem. Soc., Perkin Trans. 1* **1993**, 3139–3142.

(Scheme 3). All synthetic procedures resulted in diastereomeric mixtures of the caged compounds. The obtained mixtures of 1–6 were separated into the pure diastereomers by RP-HPLC on a preparative scale. The axial isomers eluted faster than the equatorial isomers. The isomeric species were assigned by <sup>31</sup>P NMR as reported for the axial and equatorial isomers of known cAMP and cGMP esters.<sup>18</sup> The <sup>31</sup>P NMR signals at high field (between  $\delta$  -5.1 and  $\delta$  -4.0) correspond to the axial isomers of 1–6 and those at low field (between  $\delta$  -3.6 and  $\delta$  -4.0) to the respective equatorial isomers. 4-(Hydroxymethyl)-7-methoxycoumarin (9) was prepared according to Sehgal and Seshadri via hydrolysis of the corresponding (coumarin-4-yl)methyl acetate.<sup>19</sup> The alcohol 7, previously synthesized by Dutta et al., was obtained by reduction of the corresponding aldehyde with sodium borohydride.<sup>20</sup> The unknown (hydroxymethyl)-coumarins 8 and 10 were synthesized in analogous fashion. The procedure of Sehgal and Seshadri failed for the synthesis of both 7-(dialkylamino)-4-(hydroxymethyl)-coumarins 11 and 12. These compounds were synthesized via sodium borohydride reduction of the corresponding 7-(dialkylamino)-4-formylcoumarins,<sup>20</sup> in contrast to the method previously described by Kalmykova et al.<sup>21</sup> for 7-(diethylamino)-4-(hydroxymethyl)coumarin (12).

### UV/Vis Absorption and Fluorescence Spectra.

The absorption spectra of the caged compounds 1–6 are characterized by two intensive absorption bands in the region of  $\lambda = 310$ –400 nm and around  $\lambda = 260$  nm (Figure 1). The caged compounds are bichromophoric systems, and the absorption spectra reflect the superimposition of individual chromophores, with the long-wavelength absorption band originating from the coumarin chromophore and the short-wavelength absorption mainly caused by the purine base.<sup>12</sup> The long-wavelength absorption band properties of the caged compounds 1–6 are very similar to those of the corresponding alcohols 7–12 (Table 2). Therefore, the general influence of the coumarin structure on the long-wavelength absorption is discussed concerning the spectral properties of the alcohols 7–12.

The long-wavelength absorption band maximum is related to the  $\pi\pi^*$  transition. The  $n\pi^*$  state is very close to the  $\pi\pi^*$  state,<sup>10,14</sup> but the corresponding transition is not observable because of the low transition probability. In accordance, for the coumarin derivative 7 our molecular orbital calculations (ZINDO/S-CI) predict the  $n\pi^*$  transition to be the lowest in energy (Figure 2).  $S_0 \rightarrow S_1$  ( $n\pi^*$ ) is mainly characterized by the transitions HOMO - 2  $\rightarrow$  LUMO (coefficient 0.51) and HOMO - 2  $\rightarrow$  LUMO + 2 (coefficient 0.36). The specific symmetry of the *n* orbital HOMO - 2 (Figure 3a) illustrates the  $n\pi^*$  character of  $S_1$  most clearly. The weak oscillator strength ( $f = 0.0004$ ) is also in accordance with an  $n\pi^*$  transition.  $S_0 \rightarrow S_2$  ( $\pi\pi^*$ ) is dominantly characterized by the transition HOMO  $\rightarrow$  LUMO (coefficient 0.59). The HOMO and LUMO have typical  $\pi$  symmetry (Figure 3b). The calculated oscillator strength is  $f = 0.22$ , and thus, the  $\pi\pi^*$  absorption band completely masks the  $n\pi^*$  transition.

(18) Engels, J.; Schlaeger, E. J. *J. Med. Chem.* **1977**, 20, 907–911. Engels, J. *J. Bioorg. Chem.* **1979**, 8, 9–16.

(19) Sehgal, J. M.; Seshadri, T. R. *J. Sci. Ind. Res.* **1953**, 12B, 346–349.

(20) Dutta, L. N.; Bhattacharyya, M.; Sarkar, A. K. *Can. J. Chem.* **1995**, 73, 1556–1562.

(21) Kalmykova, E. A.; Kuznetsova, N. A.; Kaliya, O. L.; Tavrizova, M. A. *J. Gen. Chem. USSR* **1991**, 61, 911–916.



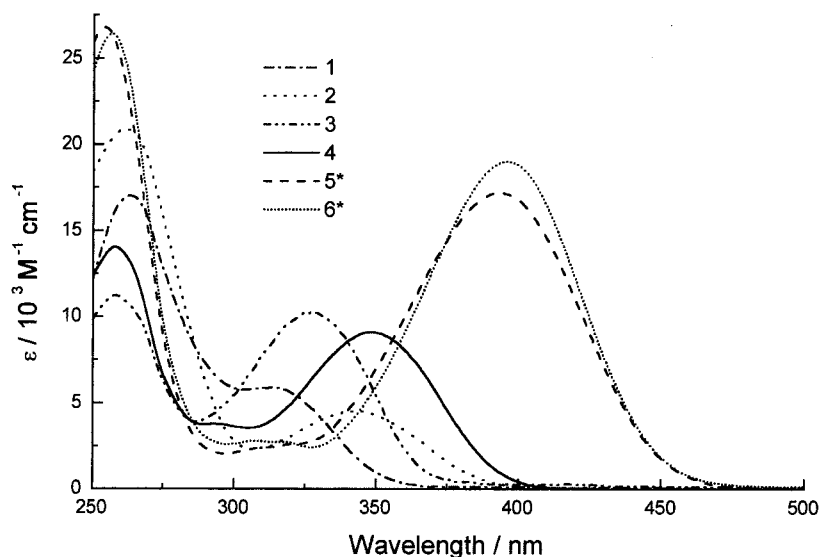


**Figure 1.** UV/vis spectra of the axial isomers of the (coumarin-4-yl)methyl-caged cAMPs in MeOH/HEPES, 1:4 (an asterisk indicates MeOH/HEPES, 1:1).

**Table 2. Properties of the Investigated Coumarinylmethyl-Caged cAMPs 1–6 and the 4-(Hydroxymethyl)coumarins 7–12 in MeOH/HEPES, 1:4<sup>a</sup>**

compound		$\lambda_{\text{abs}}^{\text{max}}/\text{nm}$ ( $\epsilon/\text{M}^{-1}\text{cm}^{-1}$ )	$\lambda_{\text{f}}^{\text{max}}/\text{nm}$	$\varphi_{\text{chem}}$	$\varphi_{\text{f}}$
CM-cAMP ( <b>1</b> )	ax	314 (5900)	396	0.085	0.0005
	eq	310 (5500)	392	0.055	0.0005
6-MCM-cAMP ( <b>2</b> )	ax	346 (4500)	450	0.03	0.008
	eq	345 (4200)	452	0.02	0.0085
7-MCM-cAMP ( <b>3</b> )	ax	328 (13200)	400.5	0.13	0.030
	eq	325 (13300)	400.5	0.07	0.040
DMCM-cAMP ( <b>4</b> )	ax	349 (11000)	444	0.04	0.021
	eq	346 (11500)	443	0.04	0.023
DMACM-cAMP ( <b>5</b> ) <sup>a</sup>	ax	394 (17200)	482	0.28	0.0085
	eq	387 (16100)	480	0.26	0.0070
DEACM-cAMP ( <b>6</b> ) <sup>a</sup>	ax	402 (18600)	483	0.21	0.0055
	eq	396 (20200)	485	0.23	0.0060
CM-OH ( <b>7</b> )		310 (5100)	397		0.005
6-MCM-OH ( <b>8</b> )		337 (4800)	465.5		0.16
7-MCM-OH ( <b>9</b> )		317 (13300)	394		0.65
DMCM-OH ( <b>10</b> )		341 (11700)	437.5		0.59
DMACM-OH ( <b>11</b> )		378 (17800)	491		0.21
DEACM-OH ( <b>12</b> )		387 (20900)	484		0.082

<sup>a</sup> In MeOH/HEPES, 1:1.

Because of the dominance of the HOMO  $\rightarrow$  LUMO transition, the influence of substituents on the long-wavelength absorption band ( $S_0 \rightarrow S_2$ ) is described approximately by structural influences on the HOMO and LUMO. Figure 3b shows the 2D contour orbital plotting (orbital squared) of the HOMO and LUMO.

To compare the spectroscopic consequences of 6- and 7-methoxy substitution on the coumarin moiety, it is necessary to compare the respective MO coefficients. The MO coefficients of the HOMO and LUMO differ much more strongly at the 6- than at the 7-position, and consequently the HOMO–LUMO energy difference, which approximately corresponds to the long-wavelength excitation energy, decreases more strongly in the case of 6-methoxy substitution as compared to 7-methoxy substitution (**8** and **9** in Figure 2). However, the influence of the methoxy substituent on the energy of the  $n\pi^*$  state is almost negligible; therefore, a state inversion takes place in the case of methoxy substitution for both **8** and **9**.

After 6,7-dimethoxy substitution (**10**) the bathochromic shift of the long-wavelength absorption band (Figure 1)

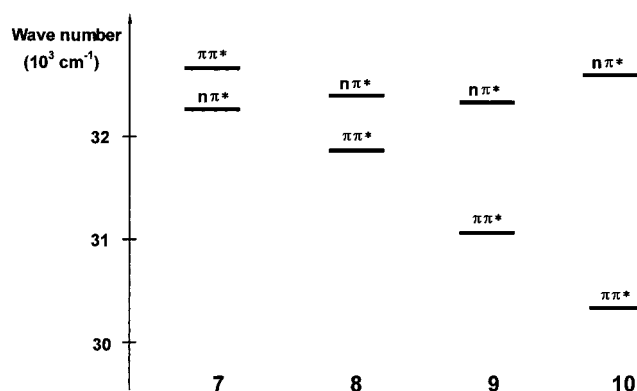


**Figure 2.** Energies of the lowest excited singlet states of 7–10 based on ZINDO/S-CI calculations.

is similar to that of **8**. The effect of the substituent in the 6-position dominates, but the extinction coefficient is about 2 times higher.

The spectroscopic properties of the 7-dialkylamino-substituted compounds **11** and **12** are qualitatively similar to those of **9**, but the stronger donor ability of the dimethylamino and the diethylamino groups causes a red shift up to the visible spectral region (Table 2) combined with increasing extinction coefficients.

The fluorescence spectra of the caged compounds **1–6** and the alcohols **7–12** (Figure 4) correspond to the respective absorption spectra. The Stokes shifts vary from 75.5 nm (equatorial isomer of **3**) to 107 nm (equatorial isomer of **2**) (Table 2). The integral fluorescence intensities of the spectra shown in Figure 4 are equivalent to the fluorescence quantum yields. Generally speaking, the absorption and fluorescence spectra of the axial and equatorial isomers of **1–6** are very similar, and no indications of a ground-state interaction between the coumarin moiety and the purine chromophore were observed.

**Deactivation Properties and Photochemistry.** The ability of the caged compounds to fluoresce is significantly lowered (Table 2). Both photochemical reaction (ester cleavage) and nonradiative deactivation (internal conversion) represent the main deactivation path-

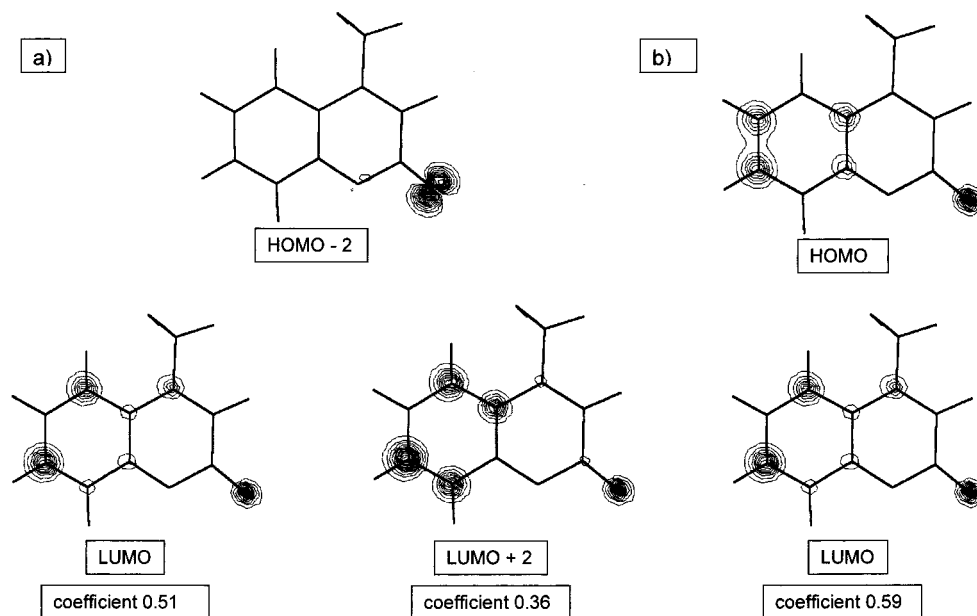


**Figure 3.** 2D contour orbital plotting (orbital squared) for the mainly participating molecular orbitals of **7**: (a)  $S_0 \rightarrow S_1$  transition ( $\text{HOMO} - 2 \rightarrow \text{LUMO}$  and  $\text{HOMO} - 2 \rightarrow \text{LUMO} + 2$ ), (b)  $S_0 \rightarrow S_2$  transition ( $\text{HOMO} \rightarrow \text{LUMO}$ ).

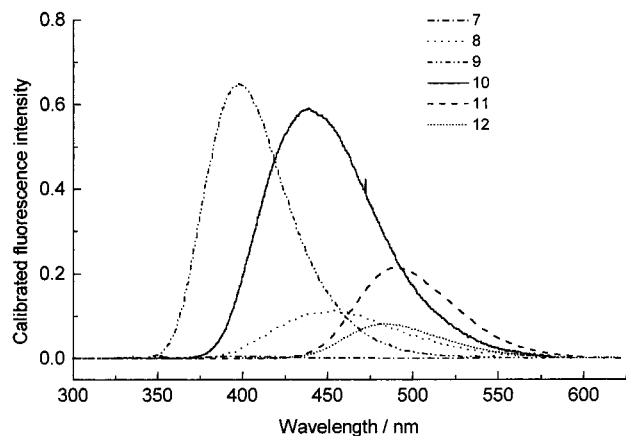


**Figure 4.** Fluorescence spectra of the photochemically liberated coumarinylmethyl alcohols **7–12** in MeOH/HEPES, 1:4.

ways of the singlet excited states. In accordance with previous results,<sup>6,10,16</sup> no indications of a significant triplet-state population were found. Therefore, an intersystem crossing process as shown in Figure 1 does not play a significant role in describing the deactivation behavior.

The fluorescence quantum yields  $\varphi_f$  of the alcohols **7–12** are up to 2 magnitudes higher than those of the caged compounds. The significantly lower value for the unsubstituted coumarinylmethyl alcohol **7** is the result of the lower energy, fluorescing  $n\pi^*$  state (Figure 2), causing a decreased radiative rate constant  $k_f$ . In this case the fluorescence cannot compete successfully with the internal conversion. An estimation of  $k_f$  using eq 1 was not possible because the fluorescence decay time  $\tau_f$  was too short to be measured with the equipment used.

$$k_f = (\tau_f^n)^{-1} = \varphi_f(\tau_f)^{-1} \quad (1)$$

Table 1 shows the decay times  $\tau_f$ , the radiative lifetimes  $\tau_f^n$ , and the radiative rate constants  $k_f$  for the alcohols investigated. Apart from that of **7** discussed above, the radiative rate constant for **8** is the smallest. This pho-

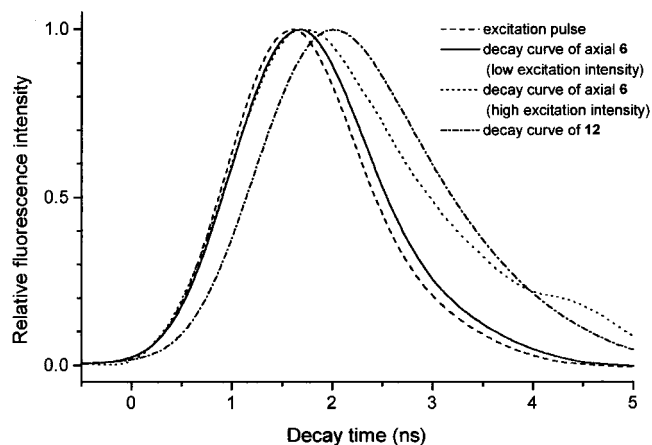


**Figure 5.** Fluorescence decay curves of **6** and of the liberated alcohol **12**.

kinetic property is in agreement with its minimal transition probability (extinction coefficient) according to the *Strickler–Berg* equation.<sup>22</sup>

On photolysis of the caged compounds, only the formation of cAMP and the corresponding coumarinylmethyl alcohol may be observed quantitatively. In analogy to previously discussed coumarinylmethyl-caged compounds,<sup>6,10</sup> the mechanism of the photolytic ester cleavage ( $\text{photo-S}_{\text{N}}1$ ) is described in Scheme 1. Information concerning the magnitude of the rate constant of the product formation can be gleaned from the fluorescence decay curves of the caged compounds after single-pulse photolysis. In Figure 5 the fluorescence decay curves of **6** and of the corresponding alcohol **12** are shown together with the time profile of the response function of the laser/detection system used. At low excitation intensity the fluorescence decay curve of the caged compound **6** (axial isomer) follows the single-exponential decay law. The time delay is relatively very close to the response function, and an exact deconvolution is not possible because

of the limited time resolution of the equipment (less than 200 ps). High-intensity pulse photolysis of the axial isomer **6** produces a more complex decay curve. In the first time interval (0–2 ns), the low- and high-intensity decay curves are very similar and are determined by the kinetics of the weak fluorescence of the caged compound. In the second interval (2 ns and later) an additional fluorescence signal appears, prolonging the global fluorescence decay. The delay of the fluorescence decay (high-intensity excitation) corresponds with the fluorescence decay curve of the alcohol **12** (Figure 5). The complex fluorescence decay behavior is the result of the formation of the strong fluorescent alcohol during the laser pulse and the excitation of the liberated alcohol by the same (actinic) laser pulse. The observed delay increases with the single-pulse intensity. Considering the pulse duration, the rate constant of the formation of the coumarinylmethyl alcohols **7–12** and, therefore, of the liberation of the cyclic nucleotide cAMP is about  $10^9 \text{ s}^{-1}$ .

The photochemical ester cleavage of the [(dialkylamino)coumarinyl]methyl-caged compounds **5** and **6** is more efficient than the photolysis of the other compounds investigated (compare the photochemical quantum yields in Table 2). Following the reaction pathway shown in Scheme 1, the photochemical quantum yield is determined by (a) the ratio of the rate constants of the competing photophysical deactivation on the depopulation of the singlet excited state (fluorescence and nonradiative,  $k_f^n$  and  $k_{nr}$ ) and bond heterolysis ( $k_1$ ) and (b) the competition of the ion pair recombination ( $k_0$ ) and the escape process ( $k_{esc}$ ). On stabilization of the intermediately formed carbocation  $\text{Cou-CH}_2^+$  by electron donor groups, the recombination ( $k_0$ ) is less efficient and the escape process ( $k_{esc}$ ) whereby cAMP and the corresponding alcohol are formed predominates.

The decreased photoreactivity of **2** and **4** compared with **1** and **3** probably results from the low-lying  $S_1$  state (compare  $\varphi_{chem}$  and  $\lambda_f$  in Table 2). In this case the energy gap between the excited-state  $S_1$  and the ion pair state  $[\text{Cou-CH}_2^+ \text{-OH}]$  is less exergonic, decreasing  $k_1$  and reducing the ratio  $k_1/(k_f^n + k_{nr})$ .

### Conclusions

Depending on the chemical structure of the coumarinylmethyl caging group (R, R'), the caged cAMPs can be excited in a wavelength region from 300 up to 450 nm. Using specific donor substituents in defined positions, it is possible to tune the absorbance to given excitation wavelengths (light source). The moderate fluorescence properties of the caged compounds in comparison with the corresponding strongly fluorescent 4-(hydroxymethyl)coumarin photoproducts allow the indirect estimation of the amount of photolytically released cyclic nucleotides in aqueous buffer solutions using fluorescence measurements. The rate constant of the liberation of cAMP is on the nanosecond (**3**, **4**) or subnanosecond (**5**, **6**) time scale, and therefore orders of magnitude less than 1 ms (rise time of well-known *o*-nitrobenzyl-caged compounds).<sup>1e,h,4c</sup> These ultrafast jumps in the biological activity can be used for studying fast physiological responses.

### Experimental Section

**Materials and Methods.** Phenol, 4-hydroxyanisole, 4-(bromomethyl)-7-methoxycoumarin, 4-(bromomethyl)-6,7-dimethoxycoumarin, 7-(dimethylamino)-4-methylcoumarin, cAMP, and

$\text{SeO}_2$  were purchased from Sigma (Germany). 7-(Diethylamino)-4-methylcoumarin, *p*-toluenesulfonyl hydrazide, and triethylamine were obtained from Lancaster (Germany). 4-(Bromomethyl)coumarin and 4-(bromomethyl)-6-methoxycoumarin were synthesized according to Woodruff<sup>23</sup> via bromination of the 4-methyl group with NBS. 4-(Diazomethyl)-7-(diethylamino)coumarin was prepared according to Ito et al.<sup>24</sup> by  $\text{SeO}_2$  oxidation of 7-(diethylamino)-4-methylcoumarin to the corresponding coumarin-4-carbaldehyde followed by triethylamine-mediated Bamford–Stevens reaction of its tosylhydrazone. 4-(Diazomethyl)-7-(dimethylamino)coumarin was synthesized following the same procedure starting from 7-(dimethylamino)-4-methylcoumarin.

7-MCM-caged cAMP (**3**) and 7-(diethylamino)-4-(hydroxymethyl)coumarin (**12**) were prepared as previously described.<sup>10,25</sup>

TLC plates, silica 60-F254, were purchased from E. Merck (Germany). Silica gel (30–60  $\mu\text{m}$ ) for flash chromatography was from J. T. Baker (The Netherlands). Acetonitrile from Riedel-deHaën (Germany) was HPLC grade. All other chemicals and solvents were reagent grade and were used without further purification. Water was purified with a Milli-Q system (Millipore, Germany). For analytical HPLC a Hewlett-Packard HP 1100 system with DAD and fluorescence detection was used. A C18 column (Spherisorb ODS 2, 5  $\mu\text{m}$ , 250  $\times$  4 mm, Polymer Laboratories Ltd., U.K.) was used for HPLC analysis at a flow rate of 1 mL/min at 20 °C with an injection volume of 20  $\mu\text{L}$ . Preparative RP-HPLC using a Shimadzu LC-8A system with UV detection (SPD-6AV) was carried out over a PLRP-S 100-10 column (300  $\times$  25 mm, Polymer Laboratories) at a flow rate of 10 mL/min using a linear gradient of 5–45% (**1–5**) or 15–45% (**6**) over 105 min; eluent A was water, and eluent B was acetonitrile.

<sup>1</sup>H NMR spectra were recorded on a Gemini 200 spectrometer (Varian) using TMS as internal standard. <sup>31</sup>P NMR spectra were recorded using a Bruker DRX 600 spectrometer with 85% phosphoric acid as external standard.

ESI mass spectrometry was performed on a triple quadrupole instrument (TSQ 700, Finnigan MAT, Germany) equipped with an electrospray ion source (API-ESI) operating in the positive mode with a capillary temperature of 200 °C at a voltage of 4.5 kV.

All melting points are uncorrected.

### Syntheses. (Coumarin-4-yl)methyl Adenosine Cyclic 3',5'-Monophosphate (**1**).

**Via the Tetra-*n*-butylammonium Salt Procedure (Method A).** A mixture of 497 mg (2 mmol) of **13** and 606.8 mg (1 mmol) of the dihydrate of the tetra-*n*-butylammonium salt of cAMP (prepared from cAMP via ion exchange with tetra-*n*-butylammonium hydroxide) was refluxed in 50 mL of acetonitrile in the dark for 5 h. The solvent was evaporated in vacuo, and the residue was washed with 20 mL of water, dried, and dissolved in chloroform/methanol. The mixture was purified by flash chromatography. Elution using chloroform/methanol (19:1 to 4:1, v/v) yielded 140 mg (28.9%) of the diastereomeric mixture of **2** in an 85:15 ratio (axial/equatorial) as a colorless solid after evaporation and lyophilization. Preparative RP-HPLC permitted separation of the axial and equatorial isomers.

**Via the Silver(I) Oxide Procedure (Method B).** A mixture of 197.5 mg (0.6 mmol) of cAMP and 447 mg (1.8 mmol) of **13** was stirred in 5 mL of DMSO and 30 mL of acetonitrile in the dark. After addition of 277.7 mg (1.2 mmol) of silver(I) oxide the resulting black suspension was stirred at 60 °C in the dark for 45 h. The reaction mixture was filtered and washed with chloroform. The combined filtrates were evaporated under reduced pressure. DMSO was removed by repeated extraction with ether. The residue was purified by flash chromatography. Elution with chloroform/methanol (19:1

(23) Woodruff, H. In *Organic Synthesis*; Drake, N. L., Ed.; Wiley & Sons: New York, 1944; Vol. 24, pp 69–72.

(24) Ito, K.; Maruyama, J. *Chem. Pharm. Bull.* **1983**, *31* (9), 3014–3023.

(25) Schönleber, R. O.; Bendig, J.; Hagen, V.; Giese, B. *Bioorg. Med. Chem.*, in press.



to 4:1, v/v) yielded 74.5 mg (25.5%) of the diastereomeric mixture of **1** in a 57:43 ratio (axial/equatorial) as a colorless solid after evaporation and lyophilization. The axial and equatorial isomers were separated from each other by preparative RP-HPLC.

**Data for axial (coumarin-4-yl)methyl cAMP (axial 1):** TLC  $R_f$  0.55 (chloroform/methanol, 5:1, v/v);  $^{31}\text{P}$  NMR (DMSO- $d_6$ ) heteronuclear decoupled  $\delta$  -5.06;  $^1\text{H}$  NMR (DMSO- $d_6$ )  $\delta$  4.30 (1H, dt,  $J$  = 10.0 and 5.0 Hz), 4.48 (1H, t,  $J$  = 10.0 Hz), 4.52–4.55 (1H, m), 4.65–4.76 (2H, m), 5.39 (1H, dd,  $J$  = 10.0 and 5.0 Hz), 5.52 (1H, d,  $J$  = 6.0 Hz), 6.07 (1H, s), 6.40 (1H, d,  $J$  = 7 Hz), 6.68 (1H, s), 7.35–7.42 (3H, m), 7.48 (1H, d,  $J$  = 8.2 Hz), 7.67 (1H, t,  $J$  = 8.3 Hz), 7.81 (1H, d,  $J$  = 7.7 Hz), 8.10 (1H, s), 8.34 (1H, s); ESI MS  $m/e$  488.3 [M + H] $^+$ . Anal. Calcd for  $\text{C}_{20}\text{H}_{18}\text{N}_5\text{O}_8\text{P}\cdot\text{H}_2\text{O}$  (505.38): C, 47.53; H, 3.99; N, 13.86. Found: C, 47.44; H, 3.80; N, 13.30.

**Data for equatorial (coumarin-4-yl)methyl cAMP (equatorial 1):** TLC  $R_f$  0.53 (chloroform/methanol, 5:1, v/v);  $^{31}\text{P}$  NMR (DMSO- $d_6$ ) heteronuclear decoupled  $\delta$  -3.66;  $^1\text{H}$  NMR (DMSO- $d_6$ )  $\delta$  4.09 (1H, dt,  $J$  = 11.0 and 5.5 Hz), 4.31 (1H, t,  $J$  = 11.0 Hz), 4.55–4.77 (3H, m), 5.38 (1H, dd,  $J$  = 10.0 and 5.5 Hz), 5.48 (1H, t,  $J$  = 6.4 Hz), 6.09 (1H, s), 6.37 (1H, s), 6.57 (1H, s), 7.36 (2H, br s), 7.42–7.48 (2H, m), 7.68 (1H, t,  $J$  = 7.8 Hz), 7.78 (1H, d,  $J$  = 7.8 Hz), 8.26 (1H, s), 8.39 (1H, s); ESI MS  $m/e$  488.2 [M + H] $^+$ . Anal. Calcd for  $\text{C}_{20}\text{H}_{18}\text{N}_5\text{O}_8\text{P}\cdot\text{H}_2\text{O}$  (505.38): C, 47.53; H, 3.99; N, 13.86. Found: C, 47.31; H, 3.72; N, 13.52.

**(6-Methoxycoumarin-4-yl)methyl Adenosine Cyclic 3',5'-Monophosphate (2).** This compound was synthesized following the same procedures previously described for **1** from **14** (537 mg, 2 mmol) and the dihydrate of the tetra-*n*-butylammonium salt of cAMP (608 mg, 1 mmol) or from cAMP (197.5 mg, 0.6 mmol), **14** (483 mg, 1.2 mmol), and silver(I) oxide (277.7 mg, 1.2 mmol). Method A yielded 161 mg (31.3%) of the diastereomeric mixture of **2** in an 85:15 ratio (axial/equatorial) as a colorless solid after evaporation and lyophilization. On the other hand, method B yielded 75 mg (25.3%, axial: equatorial = 55:45).

**Data for axial (6-methoxycoumarin-4-yl)methyl cAMP (axial 2):** TLC  $R_f$  0.64 (chloroform/methanol, 5:1, v/v);  $^{31}\text{P}$  NMR (DMSO- $d_6$ ) heteronuclear decoupled  $\delta$  -5.04;  $^1\text{H}$  NMR (DMSO- $d_6$ )  $\delta$  3.83 (3H, s), 4.30 (1H, dt,  $J$  = 10.0 and 5.0 Hz), 4.49 (1H, t,  $J$  = 10.0 Hz), 4.70–4.75 (2H, m), 5.41 (1H, dd,  $J$  = 10.0 and 4.0 Hz), 5.53 (2H, d,  $J$  = 6.0 Hz), 6.07 (1H, s), 6.41 (1H, d,  $J$  = 4.2 Hz), 6.67 (1H, s), 7.25–7.28 (2H, m), 7.35 (2H, br s), 7.43 (1H, d,  $J$  = 8.9 Hz), 8.09 (1H, s), 8.34 (1H, s); ESI MS  $m/e$  518.4 [M + H] $^+$ . Anal. Calcd for  $\text{C}_{21}\text{H}_{20}\text{N}_5\text{O}_9\text{P}\cdot\text{H}_2\text{O}$  (535.41): C, 47.11; H, 4.14; N, 13.08. Found: C, 47.44; H, 3.76; N, 13.26.

**Data for equatorial (6-methoxycoumarin-4-yl)methyl cAMP (equatorial 2):** TLC  $R_f$  0.62 (chloroform/methanol, 5:1, v/v);  $^{31}\text{P}$  NMR (DMSO- $d_6$ ) heteronuclear decoupled  $\delta$  -3.50;  $^1\text{H}$  NMR (DMSO- $d_6$ )  $\delta$  3.86 (3H, s), 4.51–4.54 (2H, m), 4.72 (1H, t,  $J$  = 5.0 Hz), 4.76–4.79 (1H, m), 5.37 (1H, q,  $J$  = 5.0 Hz), 5.47–5.49 (2H, m), 6.09 (1H, s), 6.36 (1H, s), 6.56 (1H, s), 7.22 (1H, d,  $J$  = 2.6 Hz), 7.28 (1H, dd,  $J$  = 9.1 and 2.7 Hz), 7.36 (2H, br s), 7.42 (1H, d,  $J$  = 9.0 Hz), 8.19 (1H, s), 8.39 (1H, s); ESI MS  $m/e$  518.3 [M + H] $^+$ . Anal. Calcd for  $\text{C}_{21}\text{H}_{20}\text{N}_5\text{O}_9\text{P}\cdot\text{H}_2\text{O}$  (535.41): C, 47.11; H, 4.14; N, 13.08. Found: C, 46.94; H, 3.85; N, 13.21.

**(6,7-Dimethoxycoumarin-4-yl)methyl Adenosine Cyclic 3',5'-Monophosphate (4).**

Following the same procedures described above for **1**, this compound was synthesized by reaction of **16** (448.6 mg, 1.5 mmol) with the dihydrate of the tetra-*n*-butylammonium salt of cAMP (303.4 mg, 0.5 mmol) or from cAMP (164.6 mg, 0.5 mmol), **16** (448.6 mg, 1.5 mmol), and silver(I) oxide (231.8 mg, 1.0 mmol).

Method A yielded 175 mg (approximately 57.3%) and method B 57 mg (approximately 18.7%) of a mixture of the two diastereomers after flash chromatography and lyophilization. The isomers were formed in an 85:15 ratio (axial/equatorial) (method A) and in a 55:45 ratio (method B).

**Data for axial (6,7-dimethoxycoumarin-4-yl)methyl cAMP (axial 4):** TLC  $R_f$  0.59 (chloroform/methanol, 5:1, v/v);

$^{31}\text{P}$  NMR (DMSO- $d_6$ ) heteronuclear decoupled  $\delta$  -4.99;  $^1\text{H}$  NMR (DMSO- $d_6$ )  $\delta$  3.86 (3H, s), 3.88 (3H, s), 4.30 (1H, dt,  $J$  = 10.0 and 5.0 Hz), 4.48 (1H, t,  $J$  = 10.0 Hz), 4.69–4.76 (2H, m), 5.41 (1H, dd,  $J$  = 10.0 and 5.0 Hz), 5.51 (2H, d,  $J$  = 6.0 Hz), 6.07 (s, 1H), 6.40 (1H, d,  $J$  = 5.0 Hz), 6.49 (1H, s), 7.15 (1H, s), 7.19 (1H, s), 7.35 (2H, s), 8.11 (1H, s), 8.35 (1H, s); ESI MS 548.2 [M + H] $^+$ . Anal. Calcd for  $\text{C}_{22}\text{H}_{22}\text{N}_5\text{O}_{10}\text{P}\cdot 3\text{H}_2\text{O}$  (601.46): C, 43.93; H, 4.69; N, 11.64. Found: C, 44.10; H, 4.43; N, 11.22.

**Data for equatorial (6,7-dimethoxycoumarin-4-yl)-methyl cAMP (equatorial 4):** TLC  $R_f$  0.58 (chloroform/methanol, 5:1, v/v);  $^{31}\text{P}$  NMR (DMSO- $d_6$ ) heteronuclear decoupled  $\delta$  -3.32;  $^1\text{H}$  NMR (DMSO- $d_6$ )  $\delta$  3.86 (3H, s), 3.88 (3H, s), 4.50–4.55 (2H, m), 4.71 (1H, t,  $J$  = 4.0 Hz), 4.76–4.79 (1H, m), 5.36–5.38 (1H, m), 5.46 (2H, d,  $J$  = 7.0 Hz), 6.09 (1H, s), 6.38–6.39 (2H, m), 7.13 (1H, s), 7.16 (1H, s), 7.38 (2H, s), 8.20 (1H, s), 8.39 (1H, s); ESI MS 548.2 [M + H] $^+$ . Anal. Calcd for  $\text{C}_{22}\text{H}_{22}\text{N}_5\text{O}_{10}\text{P}\cdot 4\text{H}_2\text{O}$  (619.48): C, 42.66; H, 4.88; N, 11.31. Found: C, 42.28; H, 4.36; N, 10.81.

**[7-(Dimethylamino)coumarin-4-yl]methyl Adenosine Cyclic 3',5'-Monophosphate (5).**

A mixture of 114.6 mg (0.5 mmol) of 4-(diazomethyl)-7-(dimethylamino)coumarin (**17**) and 164.6 mg (0.5 mmol) of the free acid of cAMP was stirred in 10 mL of acetonitrile and 10 mL of DMSO at 60 °C in the dark for 7 h. An additional quantity (114.6 mg, 0.5 mmol) of the diazo compound **17** was added, and the mixture was stirred at 60 °C for a further 17 h. Acetonitrile was evaporated under reduced pressure, and DMSO was removed by repeated extraction with ether/pentane (1:1). The residue which contained the axial and the equatorial isomers of **5** in a 48:52 ratio was dissolved in a small volume of chloroform/methanol (1:1, v/v) and separated by flash chromatography on a silica gel column. Elution with methanol/chloroform (1:24, v/v) and methanol/chloroform (2:23, v/v) gave fractions containing mixtures of the axial and the equatorial isomers of **5**. The fractions were dried on a rotary evaporator. Lyophilization yielded mixtures of the two isomers of **5** (44.5 mg, 16.0%) as solids. The axial and equatorial isomers were purified by preparative RP-HPLC.

**Data for axial [7-(dimethylamino)coumarin-4-yl]-methyl cAMP (axial 5):** TLC  $R_f$  0.61 (chloroform/methanol, 5:1, v/v);  $^{31}\text{P}$  NMR (DMSO- $d_6$ ) heteronuclear decoupled  $\delta$  -4.96;  $^1\text{H}$  NMR (DMSO- $d_6$ )  $\delta$  3.02 (6H, s), 4.28 (1H, dt,  $J$  = 10.0 and 4.0 Hz), 4.42 (1H, t,  $J$  = 10.0 Hz), 4.67–4.72 (2H, m), 5.38 (1H, dd,  $J$  = 9.0 and 5.0 Hz), 5.41 (2H, d,  $J$  = 7.0 Hz), 6.03 (1H, s), 6.26 (1H, s), 6.39 (1H, d,  $J$  = 4.0 Hz), 6.61 (1H, d,  $J$  = 2.0 Hz), 6.71 (1H, dd,  $J$  = 9.0 and 2.0 Hz), 7.35 (2H, s), 7.56 (1H, d,  $J$  = 9.0 Hz), 8.11 (1H, s), 8.34 (1H, s); ESI MS 531.3 [M + H] $^+$ . Anal. Calcd for  $\text{C}_{22}\text{H}_{23}\text{N}_6\text{O}_8\text{P}\cdot\text{H}_2\text{O}$  (548.45): C, 48.18; H, 4.59; N, 15.32. Found: C, 48.51; H, 4.33; N, 15.20.

**Data for equatorial [7-(dimethylamino)coumarin-4-yl]-methyl cAMP (equatorial 5):** TLC  $R_f$  0.59 (chloroform/methanol, 5:1, v/v);  $^{31}\text{P}$  NMR (DMSO- $d_6$ ) heteronuclear decoupled  $\delta$  -3.50;  $^1\text{H}$  NMR (DMSO- $d_6$ )  $\delta$  3.03 (6H, s), 4.49–4.52 (2H, m), 4.72 (1H, t,  $J$  = 5.0 Hz), 4.73–4.77 (1H, m), 5.34–5.38 (3H, m), 6.09 (1H, s), 6.15 (1H, s), 6.37 (1H, d,  $J$  = 4.0 Hz), 6.61 (1H, d,  $J$  = 2.0 Hz), 6.76 (1H, dd,  $J$  = 9.0 and 4.0 Hz), 7.36 (2H, s), 7.52 (1H, d,  $J$  = 9.0 Hz), 8.19 (1H, s), 8.39 (1H, s); ESI MS 531.4 [M + H] $^+$ . Anal. Calcd for  $\text{C}_{22}\text{H}_{23}\text{N}_6\text{O}_8\text{P}\cdot 2\text{H}_2\text{O}$  (566.46): C, 46.65; H, 4.80; N, 14.84. Found: C, 46.68; H, 4.65; N, 14.37.

**[7-(Diethylamino)coumarin-4-yl]methyl Adenosine Cyclic 3',5'-Monophosphate (6).** Following the same procedure described above for **5**, this compound was synthesized from the free acid of cAMP (164.6 mg, 0.5 mmol) and 4-(diazomethyl)-7-(diethylamino)coumarin (**18**) (257.3 mg, 1 mmol) in 16 mL of acetonitrile and 4 mL of DMSO.

A 59 mg yield of a mixture of the two isomers of **6** was obtained after flash chromatography and lyophilization. The yield was 20.5%, and the isomers were formed in a 45:55 ratio (axial/equatorial). Preparative RP-HPLC as described for **5** permitted separation of the axial form from the equatorial form.

**Data for axial [7-(diethylamino)coumarin-4-yl]methyl cAMP (axial 6):** TLC  $R_f$  0.86 (chloroform/methanol, 5:1, v/v);

<sup>31</sup>P NMR (DMSO-*d*<sub>6</sub>) heteronuclear decoupled  $\delta$  -4.96; <sup>1</sup>H NMR (DMSO-*d*<sub>6</sub>)  $\delta$  1.10 (6H, t,  $J$  = 7.0 Hz), 3.42 (4H, q,  $J$  = 7.0 Hz), 4.28 (1H, dt,  $J$  = 10.0 and 5.0 Hz), 4.41 (1H, t,  $J$  = 10.0 Hz), 4.66–4.72 (2H, m), 5.37–5.41 (3H, m), 6.06 (1H, s), 6.22 (1H, s), 6.37 (1H, d,  $J$  = 4.0 Hz), 6.57 (1H, d,  $J$  = 2.0 Hz), 6.66 (1H, dd,  $J$  = 9.0 and 2.0 Hz), 7.34 (2H, s), 7.53 (1H, d,  $J$  = 9.0 Hz), 8.12 (1H, s), 8.33 (1H, s); ESI MS 559.3 [M + H]<sup>+</sup>. Anal. Calcd for C<sub>24</sub>H<sub>27</sub>N<sub>6</sub>O<sub>8</sub>P·H<sub>2</sub>O (576.50): C, 50.00; H, 5.07; N, 14.58. Found: C, 49.70; H, 4.78; N, 14.09.

**Data for equatorial [7-(diethylamino)coumarin-4-yl]-methyl cAMP (equatorial 6):** TLC  $R_f$  0.84 (chloroform/methanol, 5:1, v/v); <sup>31</sup>P NMR (DMSO-*d*<sub>6</sub>) heteronuclear decoupled  $\delta$  -3.51; <sup>1</sup>H NMR (DMSO-*d*<sub>6</sub>)  $\delta$  1.13 (6H, t,  $J$  = 7.0 Hz), 3.45 (4H, q,  $J$  = 7.0 Hz), 4.50–4.53 (2H, m), 4.71 (1H, t,  $J$  = 5.0 Hz), 4.75 (1H, d,  $J$  = 12.0 Hz), 5.34–5.35 (3H, m), 6.08 (1H, s), 6.11 (1H, s), 6.36 (1H, d,  $J$  = 4.0 Hz), 6.56 (1H, d,  $J$  = 2.0 Hz), 6.72 (1H, dd,  $J$  = 9.0 and 3.0 Hz), 7.35 (2H, s), 7.49 (1H, d,  $J$  = 9.0 Hz), 8.19 (1H, s), 8.39 (1H, s); ESI MS 559.4 [M + H]<sup>+</sup>. Anal. Calcd for C<sub>24</sub>H<sub>27</sub>N<sub>6</sub>O<sub>8</sub>P·H<sub>2</sub>O (576.50): C, 50.00; H, 5.07; N, 14.58. Found: C, 49.89; H, 4.74; N, 14.04.

**4-(Hydroxymethyl)coumarin (7).** A mixture of 1.6 g (6.7 mmol) of **13** and 5.5 g (67 mmol) of sodium acetate in 30 mL of acetic anhydride was refluxed for 4 h. After filtration and washing of the residue with 20 mL of boiling acetic anhydride, the resulting filtrate was poured into ice-water after being cooled. The resulting white precipitate of 4-(acetoxymethyl)-coumarin was refluxed in 100 mL of a mixture of ethanol and hydrochloric acid (1:1) for 2 h. After the reaction mixture was cooled to room temperature, it yielded 0.8 g (71%) of **7** as a colorless solid: mp 136 °C; NMR data available in ref 23; ESI MS 177.2 [M + H]<sup>+</sup>. Anal. Calcd for C<sub>10</sub>H<sub>8</sub>O<sub>3</sub> (176.17): C, 68.18; H, 4.58. Found: C, 67.86; H, 4.56.

**4-(Hydroxymethyl)-6-methoxycoumarin (8).** Following the same procedure described above for **7**, this compound was synthesized from 1.8 g (6.7 mmol) of **14**. The yield was 590 mg (64%): mp 183 °C; <sup>1</sup>H NMR (CDCl<sub>3</sub>)  $\delta$  3.85 (3H, s), 4.90 (2H, s), 6.64 (1H, s), 6.93 (1H, d,  $J$  = 3 Hz), 7.11 (1H, dd,  $J$  = 9.0 and 3.0 Hz), 7.30 (1H, d,  $J$  = 4.2 Hz); ESI MS 207.4 [M + H]<sup>+</sup>. Anal. Calcd for C<sub>11</sub>H<sub>10</sub>O<sub>4</sub> (206.20): C, 64.07; H, 4.89. Found: C, 63.89; H, 4.74.

**6,7-Dimethoxy-4-(hydroxymethyl)coumarin (10).** Compound **10** was synthesized as described for **7** from 2 g (6.7 mmol) of **16**. The reaction yielded 1.138 g (72%) of **10**: mp 188 °C;

<sup>1</sup>H NMR (CDCl<sub>3</sub>)  $\delta$  3.90 (3H, s), 3.92 (3H, s), 4.85 (2H, s), 6.46 (1H, s), 6.82 (1H, s), 6.88 (1H, s); ESI MS 237.0 [M + H]<sup>+</sup>. Anal. Calcd for C<sub>12</sub>H<sub>12</sub>O<sub>5</sub> (236.22): C, 61.01; H, 5.12. Found: C, 60.47; H, 5.01.

**7-(Dimethylamino)-4-(hydroxymethyl)coumarin (11).** A mixture of 1.77 g (8.1 mmol) of 7-(dimethylamino)coumarin-4-carbaldehyde and 587 mg (15.5 mmol) of sodium borohydride in 50 mL of THF and 50 mL of 2-propanol was refluxed overnight. After decomposition of borohydride by addition of hydrochloric acid (1 M) and following neutralization, the organic solvents were removed in vacuo. After extraction with chloroform, drying, and purification via flash chromatography (elution with chloroform), 910 mg (51%) of an orange-yellow solid was obtained: mp 175–185 °C; <sup>1</sup>H NMR (CDCl<sub>3</sub>)  $\delta$  3.03 (6H, s), 4.64 (2H, s), 5.95 (1H, s), 6.47 (1H, d,  $J$  = 2.5 Hz), 6.60 (1H, dd,  $J$  = 8.9 and 2.6 Hz), 7.35–7.40 (1H, m); ESI MS 220.1 [M + H]<sup>+</sup>. Anal. Calcd for C<sub>12</sub>H<sub>13</sub>NO<sub>3</sub> (219.24): C, 65.74; H, 5.98; N, 6.39. Found: C, 65.24; H, 5.98; N, 6.41.

**UV/Vis Spectroscopy, Photolysis Experiments, and Measurements of the Photochemical Quantum Yields.** UV/vis spectra were recorded on a U-3410 spectrophotometer (Hitachi, Japan). Photolysis was carried out using a high-pressure mercury lamp (HBO 500, Oriel) with controlled light intensity and metal interference filters (Schott, Germany) of 313 nm (**1**), 333 nm (**2–4**), and 365 nm (**5**, **6**). The irradiated solutions were analyzed by HPLC for quantum yield determinations. Solutions (50  $\mu$ M) of the caged compounds in

aqueous HEPES buffer solution (0.01 M HEPES/NaOH, 0.12 M NaCl, 3 mM KCl, 1 mM CaCl<sub>2</sub>, 1 mM MgCl<sub>2</sub>, pH 7.2)/30% acetonitrile or 20% methanol were placed in quartz cuvettes with a path length of 1 cm and irradiated for periods ranging from 3 to 90 s in steps of 3–10 s. Before and after each irradiation, the absorption spectra were recorded and the concentrations of the remaining caged compounds were measured by HPLC. The photochemical quantum yields  $\Phi_{\text{chem}}$  were determined as described<sup>6</sup> using potassium ferrioxalate actinometry<sup>26</sup> according to the equation  $\Phi_{\text{chem}} = (dI/dt)I_{\text{abs}} - 1$ . The initial slope  $dI/dt$  of the experimentally obtained concentration/irradiation time function was determined directly using the HPLC peak areas of the caged compounds. The value of  $I_{\text{abs}}$  (absorbed light intensity in moles of photons per second at  $t = 0$  and at  $\lambda = 313, 333, \text{ or } 365 \text{ nm}$ ) was calculated by multiplying the absorption factor  $\alpha$  (taken from the UV spectra at  $t = 0$  and  $\lambda = 313, 333, \text{ or } 365 \text{ nm}$ ) by the light intensity of the HBO 500 exposure tool (determined using the actinometer compound). The volume  $V$  of the solution irradiated was 3 mL.

**Fluorescence Measurements.** Fluorescence spectra were measured using an MPF-2A fluorescence spectrometer (Hitachi-Perkin-Elmer) combined with a correction and digitalization unit. Solutions (10  $\mu$ M) of the compounds under investigation were placed in quartz cuvettes of path length 1 cm and excited perpendicularly.

The fluorescence quantum yields were determined at 298 K by the relative method<sup>27</sup> using quinine sulfate as a standard ( $\Phi_f = 0.545$  in 0.1 N H<sub>2</sub>SO<sub>4</sub>). The absorbance values of the solutions of the standard and the investigated compound were identical at the excitation wavelengths (313, 333, and 365 nm; see above). The different refractive indices of the solutions were taken into account.

The time-resolved fluorescence decay measurements (pulse sampling method) were performed using a nitrogen laser ( $\lambda = 337 \text{ nm}$ ) as excitation source and a transient recorder.<sup>28</sup> The fluorescence detection wavelength was  $\lambda_f = 405 \text{ nm}$  (interference filter). The fluorescence decay curves of the (photochemically stable) coumarinylmethyl alcohols were measured using the pulse sampling method (20 pulses using the same solution). The fluorescence decay curves of the caged compounds were measured on single-pulse excitation. The solution was renewed after each single-pulse photolysis.

Details of the equipment and the deconvolution procedure of the experimental decay curve are described in ref 28. The time resolution achieved was about 200 ps.

**Molecular Orbital Calculations.** Molecular orbital calculations were performed using the semiempirical method ZINDO/S-CI, a component of the HyperChem 5.1 Pro software package,<sup>29</sup> considering 10 singly excited configurations (10 occupied, 10 unoccupied). Atomic coordinates for the ZINDO/S calculations were obtained from minimum energies determined using the molecular mechanics force field method MM+. The HOMO/LUMO data in Figures 2 and 3 were taken from the spectroscopy program of the software package.

**Acknowledgment.** We thank S. Helm, B. Dekowski, and J. Lossmann for technical assistance and S. Hecht, University of California, Berkeley, for fruitful discussions. We are grateful to R. Winter for NMR, E. Krause for MS investigations, and J. Dickson for critical reading of the manuscript. We thank the Deutsche Forschungsgemeinschaft (DFG) and the Fonds der Chemischen Industrie for financial support.

JO010692P

(26) Kuhn, H. J.; Braslawsky, S. E.; Schmidt, R. *Pure Appl. Chem.* **1989**, *61*, 187–210.

(27) Demas, J. N.; Crosby, G. A. *J. Phys. Chem.* **1971**, *75*, 991–999.

(28) Grewer, C.; Brauer, H.-C. *J. Phys. Chem.* **1993**, *97*, 5001–5006.

(29) Hypercube Inc., Gainesville, FL.